Pressure-Induced Inhomogeneous Chiral-Spin Ground State in FeGe

A. Barla,[1,2*] H. Wilhelm,[3] M. K. Forthaus,[4] C. Strohm,[5] R. Rüffer,[5] M. Schmidt,[6] K. Koepernik,[7] U. K. Rößler,[7] and M. M. Abd-Elmeguid[4]

[1]*Istituto di Struttura della Materia, ISM-CNR, I-34149 Trieste, Italy*
[2]*ALBA Synchrotron Light Source, E-08290 Cerdanyola del Vallés, Barcelona, Spain*
[3]*Diamond Light Source Ltd, Chilton, Didcot, Oxfordshire OX11 0DE, United Kingdom*
[4]*II. Physikalisches Institut, Universität zu Köln, D-50937 Köln, Germany*
[5]*European Synchrotron Radiation Facility, F-38043 Grenoble, France*
[6]*Max Planck Institute for Chemical Physics of Solids, D-01187 Dresden, Germany*
[7]*IFW Dresden, Postfach 270116, D-01171 Dresden, Germany*

(Received 15 November 2013; revised manuscript received 12 May 2014; published 6 January 2015)

^{57}Fe nuclear forward scattering on the chiral magnet FeGe reveals an extremely large precursor phase region above the helimagnetic ordering temperature $T_C(p)$ and beyond the pressure-induced quantum phase transition at 19 GPa. The decrease of the magnetic hyperfine field $\langle B_{\rm hf}\rangle$ with pressure is accompanied by a large increase of the width of the distribution of $\langle B_{\rm hf}\rangle$, indicating a strong quasistatic inhomogeneity of the magnetic states in the precursor region. Hyperfine fields of the order of 4 T (equivalent to a magnetic moment $\mu_{\rm Fe} \approx 0.4\mu_B$) persist up to 28.5 GPa. No signatures of magnetic order have been found at about 31 GPa. The results, supported by *ab initio* calculations, suggest that chiral magnetic precursor phenomena, such as an inhomogeneous chiral-spin state, are vastly enlarged due to increasing spin fluctuations as FeGe is tuned to its quantum phase transition.

DOI: 10.1103/PhysRevLett.114.016803 PACS numbers: 75.30.Kz, 62.50.-p, 71.15.Mb

Increasing the lattice density of ferromagnets reveals many surprising effects close to a quantum phase transition (QPT). In Fe, the classical example of a band ferromagnet, a superconducting ground state is entered after the magnetic order is suppressed at the pressure-induced first-order structural phase transition [1,2]. However, a continuous transition from a ferromagnetic (FM) to a paramagnetic (PM) state at zero temperature with a quantum critical behavior remains elusive. So far, a pressure-induced suppression of magnetic order without a structural phase transition has been observed only in few (weakly) itinerant ferromagnets, like $ZrZn_2$ [3], MnSi [4], Ni_3Al [5], and CoS_2 [6]. They have markedly reduced magnetic moments ($\mu \lesssim 0.5\mu_B$) and low Curie temperatures ($T_C \lesssim 50$ K). The experimentally observed magnetic and transport anomalies in such systems then may be related to fluctuation-induced first-order QPTs which seem to prevail thanks to a propensity of the magnetic subsystem to couple to other low-lying soft modes [7], and/or to the evolution of complex spin structures associated with a tricritical point [8,9].

In this context, cubic FeGe and MnSi belong to a particular class of intermetallic compounds owing to their chiral helimagnetism, that is induced by weak spin-orbit coupling [10–19]. Within the phenomenological Dzyaloshinskii theory of chiral magnets [19,20] the mechanism and distinctive features of these compounds are (i) a confinement of localized chiral modulations [17,20,21] by a coupling between the (longitudinal) magnitude of the local magnetization and its orientation [22–24] and (ii) a corresponding inhomogeneity of the magnetic state. Unlike in the homogeneous helical ground state with a fixed local spin-density magnitude, the longitudinal modulus of the magnetization is strongly varying in a *precursor* region to magnetic ordering. Thus, in this case, such a region between the PM and the helical state is expected to be anomalous on fundamental grounds [17,21,22,24]. One anticipates the existence of inhomogeneous textures of the order parameter where one, two, and even three dimensional twisted configurations are possible [21,24]. In all cases the twisted spin density is associated with an inhomogeneity of the magnetization modulus that can exist as a precursor state, which is not long-range ordered but a fluid arrangement of localized twisted spin densities.

For thermally driven transitions, such confined magnetic precursor phenomena exist in a small temperature interval of a few Kelvin, that is determined by the strength of the Dzyaloshinskii-Moriya exchange [14,16,17]. In FeGe this region is over the temperature range from $T_C = 278.5$ K to $T_0 = 280$ K [17], where T_C is the Curie temperature and T_0 defines the crossover from a chiral magnetic state, which can be identified as an inhomogeneous chiral-spin (ICS) state, to the paramagnetic state. Pressure-induced QPTs in transition-metal compounds, on the other hand, are rather complex and one observes unusual ground states at or beyond the FM to PM QPT. This is indeed the case in MnSi ($T_C \approx 29$ K), where quasistatic magnetic moments display partial order [25] beyond the critical pressure ($p_c = 1.4$ GPa) and where the electrical resistivity deviates from the Landau-Fermi liquid (LFL) behavior for

$p \gg p_c$ [26]. In FeGe ($\mu_{Fe} = 1\mu_B$), the long-range magnetic order (LRMO) is suppressed at $p_c \approx 19$ GPa and also here the electrical resistivity strongly deviates from the LFL behavior in a considerably large pressure range around p_c [27]. The magnetic properties of this region are unknown. It is, thus, of great interest to investigate its magnetic character and to explore how the temperature range of magnetic precursor phenomena is influenced by enhanced spin fluctuations when FeGe is tuned by external pressure across the FM to PM QPT.

In the present Letter we have investigated the pressure-induced evolution of the FM state in FeGe across the QPT at a *microscopic* level using ^{57}Fe nuclear forward scattering (NFS) [28]. NFS is a synchrotron-based Mössbauer technique and thereby an ideal local probe to study the pressure-induced changes in the magnetic properties via the hyperfine interactions at the Fe site [37]. It provides precise, quantitative, and easily interpreted information on the longitudinal modulation of the order parameter. The experimental data reveal that the gradual suppression of the long-range-ordered helical state is accompanied by the appearance of an inhomogeneous magnetic state for $T_C(p) < T < T_0(p)$ and $p < p_c \approx 19$ GPa. The latter becomes the ground state above 19 GPa and is eventually suppressed at $p_0 = 28.5$ GPa, where FeGe becomes paramagnetic. These observations, supported by *ab initio* calculations [28], suggest that chiral magnetic precursor states are enhanced by increasing spin fluctuations near the QPT, leading to an ICS *ground state* above p_c.

NFS spectra have been taken at the Nuclear Resonance beam line ID18 and the Nuclear Resonance end station ID22N at the European Synchrotron Radiation Facility, Grenoble [28,38]. The NFS spectra were recorded at each pressure while warming up the sample from 3 K to room temperature and were analyzed with the software package MOTIF [39]. The parameters used to describe the spectra are the magnetic hyperfine field B_{hf}, which is a measure of the Fe magnetic moment, and the electric quadrupole splitting ΔE_Q, which is related to the magnitude of the electric-field gradient (EFG) at the Fe nucleus.

Figure 1(a) shows selected ^{57}Fe NFS spectra as a function of temperature at ambient pressure. The spectrum at 290 K, i.e., in the PM phase, is characteristic of unsplit nuclear levels and can be fitted with a single line, i.e., without any sizable electric quadrupole or magnetic interaction. The appearance of quantum beats at lower temperatures, below T_C, related to the splitting of the nuclear levels by hyperfine interactions, is the signature of LRMO. The spectrum at $T = 3$ K can be reproduced with a single set of hyperfine parameters ($B_{hf} = 11.5$ T, and $\Delta E_Q \approx 0.03$ mm/s), which is in agreement with conventional Mössbauer data [40,41]. In contrast, the NFS spectra recorded in the temperature range 200 K$< T \leq 250$ K cannot be described properly in terms of a single set of hyperfine parameters. Instead, a distribution of hyperfine

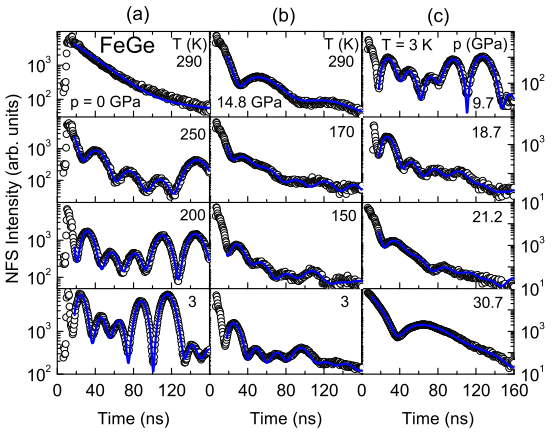

FIG. 1 (color online). Measured (open circles) and calculated (lines) ^{57}Fe NFS spectra of cubic FeGe at (a) $p = 0$, (b) 14.8 GPa and selected temperatures, and (c) $T = 3$ K at selected pressures.

parameters, approximated by two different Fe sites in the ratio of 3∶2, was used. This seems plausible as in this temperature range a first-order reorientation of the helix propagation, from the low-temperature $\langle 111 \rangle$ to the high-temperature $\langle 100 \rangle$ direction was observed at $T_2 \approx 230(15)$ K at ambient pressure [13]. In contrast to the low-temperature region, there is a distribution of angles between the Fe moments along the helix and the local EFG at each site (as this is always pointing along the local $\langle 111 \rangle$ directions) [42].

The NFS spectra up to about 10 GPa show all to have a similar behavior, as exemplified by the 3 K spectrum at 9.7 GPa [see Fig. 1(c), top panel]. From these spectra a smooth temperature dependence of the average hyperfine field $\langle B_{hf} \rangle$ is extracted, which is similar to that found at ambient pressure and is shown in Fig. 2(a), top panel. The bottom panel of Fig. 2(a) shows the temperature dependence of the NFS count rate in this low pressure range. A clear, sudden drop of the count rate by about a factor of 2 is observed at T_C for each pressure, as already observed for other compounds [43]. In first approximation, the NFS count rate is proportional to the number of nuclear scatterers contributing to each allowed nuclear transition. Below T_C, due to the presence of static Fe magnetic moments, the number of allowed nondegenerate nuclear levels increases and the number of scatterers per transition therefore decreases, with the consequent drop of the count rate. On the other hand, at T_2 the temperature dependence of the count rate does not show anomalies, as there is no variation in the number and population of nuclear levels across this transition.

A quite drastic change occurred in the spectra above 10 GPa. First, at ambient temperature, in the paramagnetic state, a measurable electric quadrupole splitting [0.35(3) mm/s at 14.8 GPa] appears. It increases up to a value of 0.42(4) mm/s at 30.7 GPa. This suggests that in this pressure range a redistribution of the electron density around

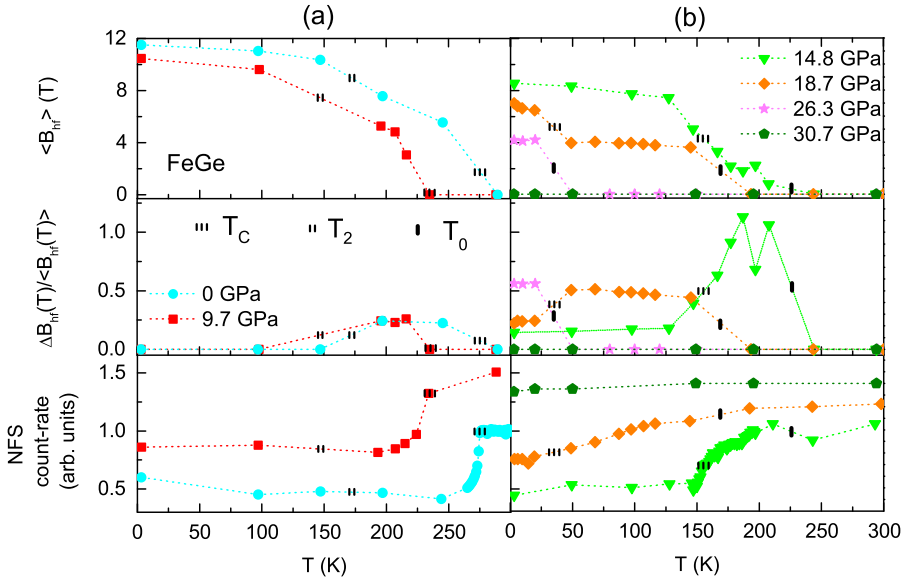

FIG. 2 (color online). Temperature dependence of the averaged hyperfine field $\langle B_{\rm hf}\rangle$ (top panel), of the relative width $\Delta B_{\rm hf}/\langle B_{\rm hf}\rangle$ of the hyperfine-field distribution (middle panel) and of the NFS count rate (bottom panel) at selected pressures (a) $p < 10$ GPa and (b) $p > 10$ GPa. The count-rate curves are all normalized to unity at room temperature and then offset for clarity when needed. The positions of $T_C(p)$, $T_2(p)$, and $T_0(p)$ are indicated in all panels by the symbols explained in the legend of the middle panel in (a).

the Fe nuclei takes place [28]. Second, the spectra at 3 K, for example the one recorded at 14.8 GPa [Fig. 1(b), bottom panel], reveal beat patterns that are washed out compared to those at lower pressures, without showing a significant acceleration of the nuclear decay.

From Fig. 2(b), top panel, it is apparent that the smooth increase of $\langle B_{\rm hf}(T)\rangle$ with decreasing temperature, observed at low pressures, has changed qualitatively at 14.8 GPa. After an initial increase, starting at $T_0(p)$, $\langle B_{\rm hf}(T)\rangle$ is almost temperature independent until a sudden rise sets in at $T_C(p) < T_0(p)$. This particular temperature variation is most prominent at 18.7 GPa. Here $\langle B_{\rm hf}(T)\rangle$ attains a constant value of about 4 T ($\mu_{\rm Fe} \approx 0.4\mu_B$) over a wide temperature interval before it strongly increases at T_C. The temperature and pressure range where this temperature independent $\langle B_{\rm hf}(T)\rangle$ is observed is identified with a new magnetic region, precursor to the LRMO state, and therefore occurring between the helical and the PM state. In contrast to the sharp decrease observed at T_C for $p < 10$ GPa, the NFS count rate [see Fig. 2(b), bottom panel] shows a gentle and continuous decrease while the temperature changes from T_0 to T_C, witnessing the slow crossover from the PM to the LRMO phase across this new state. Above $p_c \approx 19$ GPa, no LRMO was observed [27] and therefore the transition at $T_0(p)$ unambiguously reveals that this precursor phase becomes the new ground state of FeGe for $p > p_c$ [see Fig. 1(c) for the corresponding NFS spectrum at 21.2 GPa and 3 K].

The peculiar magnetic character of this precursor phase becomes evident from the width of the $\langle B_{\rm hf}(T)\rangle$ distribution [see Fig. 2(b), middle panel]. In fact, above 10 GPa, the relative width $\Delta B_{\rm hf}/\langle B_{\rm hf}\rangle$ at $T = 3$ K is about 14% at 14.8 GPa, and it increases to 22% at 18.7 GPa [these values are similar to those found for $T_2 < T < T_C$ at pressures below 10 GPa, see Fig. 2(a), middle panel]. But in the temperature range of the precursor state, the width of the average magnetic hyperfine field distribution increases enormously, up to about 100% at 14.8 GPa, and 50% at 18.7 GPa. The appearance of a narrow $B_{\rm hf}$ distribution below T_C above 10 GPa might originate from a magnetic structure implying a distribution of angles between $B_{\rm hf}$ and ΔE_Q (as is the case for the helix propagating along the $\langle 100\rangle$ directions above T_2 for $p < 10$ GPa). However, in the precursor state, which appears always above T_C, we can exclude the presence of LRMO. Therefore, the appearance of a broad $B_{\rm hf}$ distribution originates from the presence of a static distribution of Fe moments on the time scale of the nuclear Larmor precession, i.e., of the order of 10 ns [44,45]. This new state is therefore characterized by a *quasistatic* disordered spin structure that is marked by a large inhomegeneity of the local spin polarization, like in a spin liquid. Eventually, these short-range static magnetic correlations are suppressed at 30.7 GPa, where the spectra show the paramagnetic behavior for all temperatures.

Figure 3(a) displays the magnetic phase diagram of FeGe based on the NFS data (bold symbols) in conjunction with electrical resistivity data (open symbols) [27]. Both data sets show a good agreement of the pressure dependencies of T_C and T_2. The extrapolation $T_C(p) \to 0$ shows that LRMO is suppressed at $p_c \approx 19$ GPa. The precursor region deduced from the NFS data exists for $T_C(p) < T < T_0(p)$, i.e., between the helical and the PM state. $T_0(p)$ eventually

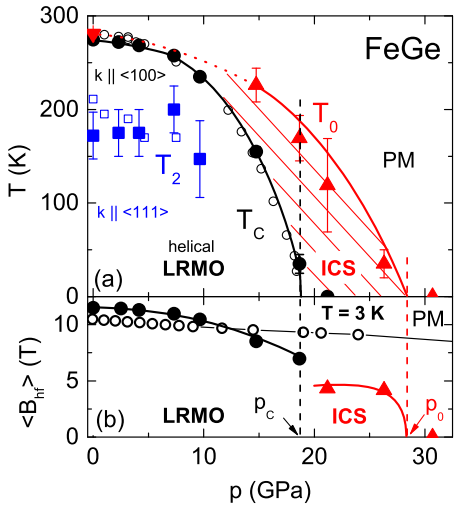

FIG. 3 (color online). (a) (T, p) phase diagram of cubic FeGe including data from transport experiments (open symbols) [27]. The long-range helical magnetic order (LRMO) sets in at T_C (black circles). The helix propagation along $\langle 100 \rangle$ changes to $\langle 111 \rangle$ below T_2 (blue squares); the point at $p = 0$ (open square) is taken from Ref. [13]. T_0 (red triangles) is the upper boundary of the phase characterized by short range magnetic correlations, which is anticipated to be an inhomogeneous chiral-spin (ICS) state. The value of T_0 at ambient pressure is taken from Ref. [17]. (b) Pressure dependence of the experimental (bold symbols, $T = 3$ K) and calculated (open symbols, $T = 0$ K) average magnetic hyperfine field. $\langle B_{\mathrm{hf}} \rangle$ values for $p \leq p_c$ and in the helical ground state are shown as black circles. Above p_c, $\langle B_{\mathrm{hf}}(p) \rangle$ (red triangles) is almost constant before it vanishes at $p_0 = 28.5(20)$ GPa.

approaches zero at $p_0 = 28.5(20)$ GPa. The pressure dependence of $\langle B_{\mathrm{hf}}(T = 3\ \mathrm{K}) \rangle$, depicted in Fig. 3(b), reflects the evolution of the ground-state magnetic moment of Fe with pressure (bold circles). In the LRMO state, $\langle B_{\mathrm{hf}}(p) \rangle$ decreases smoothly with pressure. Above p_c, however, it is nonzero and remains constant over a large pressure range [triangles in Fig. 3(b)] until it is suppressed at p_0, where the PM state is entered. In contrast to this, the calculated $B_{\mathrm{hf}}(p)$ (open circles) shows only a very gentle decrease over the pressure range covered by the experiment. Considering that the theoretical results are restricted to the zero-temperature ground state *without fluctuations*, this deviation suggests that the magnetic state for $p >$ 10 GPa is gradually affected by the enhanced fluctuations upon approaching the QPT [28].

Regarding the nature of the precursor region, we would like to point out that in cubic chiral magnets, the presence of the Dzyaloshinskii-Moriya exchange [7–9,46] not only twists the ferromagnetic spin structure into a helix, but it also causes an anomalous, thermally driven, magnetic transition. In fact, the presence of Lifshitz invariants in the phenomenological Landau-Ginzburg theory for chiral magnets [19,47] stipulates that a conventional PM-helimagnetic thermal phase transition cannot take place. This becomes evident as the transition temperature $T_C(p)$ is tuned towards zero. Upon approaching the QPT, the quantum dynamical spin fluctuations in the metallic magnets start to cooperate with the weak Dzyaloshinskii-Moriya exchange, the homogeneity of the magnetic state is destroyed, and a chiral liquidlike magnetic precursor state is expected. This state is composed of twisted and longitudinally modulated magnetic solitonic units in the form of helicoidal one-dimensional modulations or double-twisted skyrmionic cores [21,24]. The appearance of mesoscopic solitons and defects in such systems underlies their anomalous ordering transition, which is known from the occurrence of mesophases in soft matter [48].

Furthermore, we want to stress that for thermally driven transitions, such confined magnetic precursor phenomena have been detected in the $B20$ ferromagnets at ambient pressure in a small temperature interval of a few Kelvin [14,16,17,22,23]. Identifying the short-range-ordered ICS state observed below T_0 at high pressures with these precursors, we conjecture that the transition line $T_C(p)$ lies below the line $T_0(p)$ at all pressures, as depicted in Fig. 3(a). Moreover, our results show that, upon approaching the QPT, the increasing magnetic fluctuations must exacerbate the tendency of the system to stabilize such inhomogeneous magnetic textures and the precursor regime expands to an exceptionally wide temperature range. The ability of NFS to probe the magnitude and distribution of the quasistatic spin polarization yields direct microscopic evidence for the existence of the precursor state in chiral helimagnets. In a centrosymmetric itinerant magnet, however, a corresponding mechanism for longitudinal modulations and complex textures of the ordered magnetic moment does not exist. Correspondingly, evidence for spin textures with comparable features and extent near the PM-to-FM QPT has not been reported, and it is unlikely to exist, for such materials.

In conclusion, the ^{57}Fe NFS data on cubic FeGe reveal the formation of an inhomogeneous quasistatic (on a time scale of about 10 ns) magnetic state which exists up to $p_c \approx 19$ GPa for $T_C < T < T_0$ and becomes the ground state in the range $p_c < p < p_0 = 28.5(20)$ GPa for $T < T_0$. This precursor state reflects the predicted behavior of an inhomogeneous chiral-spin state composed of soliton units. Such a chiral short-range ordered precursor region, already observed at ambient pressure in FeGe, is dramatically widened by the increasing spin fluctuations near the quantum phase transition and is the origin of the observed pressure-induced wide distribution of the hyperfine fields. Furthermore, it is very likely the origin of the anomalous electronic transport behavior observed beyond p_c in FeGe and other $B20$ helimagnets, where charge carriers are scattered off these inhomogeneous and twisted spin textures.

We acknowledge fruitful discussions with A. N. Bogdanov, J. Mydosh, A. Rosch, and J. Litterst. M. M. A.

acknowledges financial support by the Deutsche Forschungsgemeinschaft (SFB 608). We thank R. Koban for technical support.

*Corresponding author.
alessandro.barla@trieste.ism.cnr.it

[1] K. Shimizu, T. Kimura, S. Furomoto, K. Takeda, K. Kontani, Y. Onuki, and K. Amaya, Nature (London) **412**, 316 (2001).
[2] C. S. Yadav, G. Seyfarth, P. Pedrazzini, H. Wilhelm, R. Černý, and D. Jaccard, Phys. Rev. B **88**, 054110 (2013).
[3] T. F. Smith, J. A. Mydosh, and E. P. Wohlfarth, Phys. Rev. Lett. **27**, 1732 (1971).
[4] J. D. Thompson, Z. Fisk, and G. G. Lonzarich, Physica (Amsterdam) **161B**, 317 (1989).
[5] P. G . Niklowitz, F. Beckers, G. G. Lonzarich, G. Knebel, B. Salce, J. Thomasson, N. Bernhoeft, D. Braithwaite, and J. Flouquet, Phys. Rev. B **72**, 024424 (2005).
[6] V. A. Sidorov, V. N. Krasnorussky, A. E. Petrova, A. N. Utyuzh, W. M. Yuhasz, T. A. Lograsso, J. D. Thompson, and S. M. Stishov, Phys. Rev. B **83**, 060412(R) (2011).
[7] D. Belitz and T. R. Kirkpatrick, Phys. Rev. Lett. **89**, 247202 (2002).
[8] T. R. Kirkpatrick and D. Belitz, Phys. Rev. B **85**, 134451 (2012).
[9] G. J. Conduit, A. G. Green, and B. D. Simons, Phys. Rev. Lett. **103**, 207201 (2009).
[10] P. Bak and M. H. Jensen, J. Phys. C **13**, L881 (1980).
[11] O. Nakanishi, A. Yanase, A. Hasegawa, and M. Kataoka, Solid State Commun. **35**, 995 (1980).
[12] S. A. Sørensen, Risø Report No. 1125.
[13] B. Lebech, J. Bernhardt, and T. Freltoft, J. Phys. Condens. Matter **1**, 6105 (1989).
[14] C. Pappas, E. Lelièvre-Berna, P. Falus, P. M. Bentley, E. Moskvin, S. Grigoriev, P. Fouquet, and B. Farago, Phys. Rev. Lett. **102**, 197202 (2009).
[15] A. Bauer, A. Neubauer, C. Franz, W. Münzer, M. Garst, and C. Pfleiderer, Phys. Rev. B **82**, 064404 (2010).
[16] S. V. Grigoriev, E. V. Moskvin, V. A. Dyadkin, D. Lamago, T. Wolf, H. Eckerlebe, and S. V. Maleyev, Phys. Rev. B **83**, 224411 (2011).
[17] H. Wilhelm, M. Baenitz, M. Schmidt, U. K. Rößler, A. A. Leonov, and A. N. Bogdanov, Phys. Rev. Lett. **107**, 127203 (2011).
[18] E. Moskvin, S. Grigoriev, V. Dyadkin, H. Eckerlebe, M. Baenitz, M. Schmidt, and H. Wilhelm, Phys. Rev. Lett. **110**, 077207 (2013).
[19] I. E. Dzyaloshinskii, Zh. Eksp. Teor. Fiz. **46**, 1420 (1964) [Sov. Phys. JETP **19**, 960 (1964)].
[20] A. N. Bogdanov and D. A. Yablonskii, Zh. Eksp. Teor. Fiz. **95**, 178 (1989) [Sov. Phys. JETP **68**, 101 (1989)].
[21] U. K. Rößler, A. N. Bogdanov, and C. Pfleiderer, Nature (London) **442**, 797 (2006).
[22] H. Wilhelm, M. Baenitz, M. Schmidt, C. Naylor, R. Lortz, U. K. Rößler, A. A. Leonov, and A. N. Bogdanov, J. Phys. Condens. Matter **24**, 294204 (2012).
[23] L. Cevey, H. Wilhelm, M. Schmidt, and R. Lortz, Phys. Status Solidi (b) **250**, 650 (2013).
[24] A. A. Leonov *et al.*, arXiv:1001.1292v3.
[25] C. Pfleiderer, D. Reznik, L. Pintschovius, H. v. Löhneysen, M. Garst, and A. Rosch, Nature (London) **427**, 227 (2004).
[26] P. Pedrazzini, D. Jaccard, G. Lapertot, J. Flouquet, Y. Inada, H. Kohara, and Y. Onuki, Physica (Amsterdam) **378B–380B**, 165 (2006).
[27] P. Pedrazzini, H. Wilhelm, D. Jaccard, T. Jarlborg, M. Schmidt, M. Hanfland, L. Akselrud, H. Q. Yuan, U. Schwarz, Yu. Grin, and F. Steglich, Phys. Rev. Lett. **98**, 047204 (2007).
[28] See Supplemental Material at http://link.aps.org/supplemental/10.1103/PhysRevLett.114.016803 for the experimental details and the *ab initio* calculations of the hyperfine parameters. This includes Refs. [29–36].
[29] H. Wilhelm, M. Schmidt, R. Cardoso-Gil, U. Burkhardt, M. Hanfland, U. Schwarz, and L. Akselrud, Sci. Tech. Adv. Mater. **8**, 416 (2007).
[30] K. Koepernik and H. Eschrig, Phys. Rev. B **59**, 1743 (1999), http://www.fplo.de.
[31] M. Neef, K. Doll, and G. Zwicknagl, Phys. Rev. B **80**, 035122 (2009).
[32] J. P. Perdew, K. Burke, and M. Ernzerhof, Phys. Rev. Lett. **77**, 3865 (1996).
[33] M. Fanciulli, A. Zenkevich, I. Wenneker, A. Svane, N. E. Christensen, and G. Weyer, Phys. Rev. B **54**, 15985 (1996).
[34] R. Wartchow, S. Geringhausen, and M. Binnewies, Z. Kristallogr. **212**, 320 (1997).
[35] L. Ortenzi, I. I. Mazin, P. Blaha, and L. Boeri, Phys. Rev. B **86**, 064437 (2012).
[36] T. Moriya, *Spin Fluctuations in Itinerant Electron Magnetism* (Springer, Heidelberg, 1985).
[37] G. Wortmann, K. Rupprecht, and H. Giefers, Hyperfine Interact. **144–145**, 103 (2002).
[38] R. Rüffer and A. I. Chumakov, Hyperfine Interact. **97–98**, 589 (1996).
[39] Yu. V. Shvyd'ko, Phys. Rev. B **59**, 9132 (1999).
[40] R. Wäppling and L. Häggström, Phys. Lett., **28A**, 173 (1968).
[41] T. Ericsson, W. Karner, L. Häggström, and K. Chandra, Phys. Scr. **23**, 1118 (1981).
[42] The cubic modification of FeGe crystalizes in the $B20$ structure (space group $P2_13$). In this structure, the atoms occupy crystallographic sites with point symmetry 3 (C_3), allowing a nonvanishing nuclear electric quadrupole and anisotropic magnetic dipole interactions. Moreover, in the chiral twisted magnetic states, a distribution of magnetically induced EFGs and angles between hyperfine fields and local EFGs is expected.
[43] A. Barla, J. P. Sanchez, J. Derr, B. Salce, G. Lapertot, J. Flouquet, B. P. Doyle, O. Leupold, R. Rüffer, M. M. Abd-Elmeguid, and R. Lengsdorf, J. Phys. Condens. Matter **17**, S837 (2005).
[44] A. Barla, J. P. Sanchez, Y. Haga, G. Lapertot, B. P. Doyle, O. Leupold, R. Rüffer, M. M. Abd-Elmeguid, R. Lengsdorf, and J. Flouquet, Phys. Rev. Lett. **92**, 066401 (2004).
[45] A. Barla, J. Derr, J. P. Sanchez, B. Salce, G. Lapertot, B. P. Doyle, R. Rüffer, R. Lengsdorf, M. M. Abd-Elmeguid, and J. Flouquet, Phys. Rev. Lett. **94**, 166401 (2005).
[46] J. Schmalian and M. Turlakov, Phys. Rev. Lett. **93**, 036405 (2004).
[47] J.-C. Tolédano and P. Tolédano, *The Landau Theory of Phase Transitions* (World Scientific, Singapore, 1987), Chap. V.
[48] D. C. Wright and N. D. Mermin, Rev. Mod. Phys. **61**, 385 (1989).